REPORT SAMSO-TR-78-18

AD A061866

DDC FILE COPY

An Investigation of Switching Behaviors of Bimetallic-Disk Thermostats

LEVEL II

Prepared by W. C. HU
Vehicle Engineering Division
Engineering Group

30 June 1978

Final Report
(April 1977-April 1978)

APPROVED FOR PUBLIC RELEASE;
DISTRIBUTION UNLIMITED

Prepared for

SPACE AND MISSILE SYSTEMS ORGANIZATION
AIR FORCE SYSTEMS COMMAND
Los Angeles Air Force Station
P.O. Box 92960, Worldway Postal Center
Los Angeles, Calif. 90009

12 04 155

DISCLAIMER NOTICE

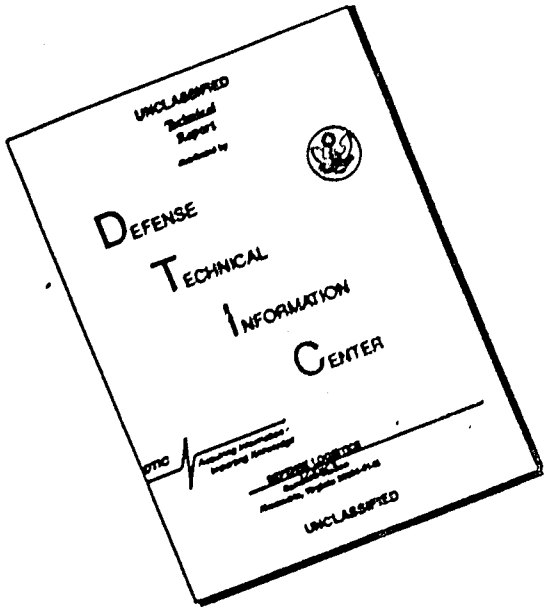

THIS DOCUMENT IS BEST QUALITY AVAILABLE. THE COPY FURNISHED TO DTIC CONTAINED A SIGNIFICANT NUMBER OF PAGES WHICH DO NOT REPRODUCE LEGIBLY.

This final report was submitted by The Aerospace Corporation, El Segundo, CA 90245, under Contract No. F04701-77-C-0078 with the Space and Missile Systems Organization, Deputy for Space Defense Systems, P. O. Box 92960, Worldway Postal Center, Los Angeles, CA 90009. It was reviewed and approved for The Aerospace Corporation by H. G. Maier, Engineering Group, and E. E. Lapin, Programs Group.

This report has been reviewed by the Information Office (OI) and is releasable to the National Technical Information Service (NTIS). At NTIS, it will be available to the general public, including foreign nations.

This technical report has been reviewed and is approved for publication. Publication of this report does not constitute Air Force approval of the report's findings or conclusions. It is published only for the exchange and stimulation of ideas.

Donald E. Hinderliter
Major, USAF

Clyde R. Magill
Lt Colonel, USAF

FOR THE COMMANDER

James E. McCormick, Col., USAF
Deputy for Space Defense System

UNCLASSIFIED

SECURITY CLASSIFICATION OF THIS PAGE (When Data Entered)

REPORT DOCUMENTATION PAGE	READ INSTRUCTIONS BEFORE COMPLETING FORM
1. REPORT NUMBER: SAMSO-TR-78-18	2. GOVT ACCESSION NO. / 3. RECIPIENT'S CATALOG NUMBER
4. TITLE (and Subtitle): AN INVESTIGATION OF SWITCHING BEHAVIORS OF BIMETALLIC-DISK THERMOSTATS	5. TYPE OF REPORT & PERIOD COVERED: Final Report, Apr 77 - Apr 78
	6. PERFORMING ORG. REPORT NUMBER: TR-0078(3409-19)-1
7. AUTHOR(s): W. C. Hu	8. CONTRACT OR GRANT NUMBER(s): F04701-77-C-0078
9. PERFORMING ORGANIZATION NAME AND ADDRESS: The Aerospace Corporation, El Segundo, Calif. 90245	10. PROGRAM ELEMENT, PROJECT, TASK AREA & WORK UNIT NUMBERS: 54p.
11. CONTROLLING OFFICE NAME AND ADDRESS: Space and Missile Systems Organization, Air Force Systems Command, Los Angeles, Calif. 90009	12. REPORT DATE: 30 June 78
	13. NUMBER OF PAGES: 54
14. MONITORING AGENCY NAME & ADDRESS (if different from Controlling Office)	15. SECURITY CLASS. (of this report): Unclassified
	15a. DECLASSIFICATION/DOWNGRADING SCHEDULE

16. DISTRIBUTION STATEMENT (of this Report)

Approved for public release; distribution unlimited.

17. DISTRIBUTION STATEMENT (of the abstract entered in Block 20, if different from Report)

18. SUPPLEMENTARY NOTES

19. KEY WORDS (Continue on reverse side if necessary and identify by block number)

Bimetallic Thermostat
Curved Disk (shallow shell)
Thermoelastic Stability
Snap-through Buckling
Switching Anomaly
Temperature Dithering
Nonlinear Boundary-Value Problem
Design Criteria

20. ABSTRACT (Continue on reverse side if necessary and identify by block number)

Thermostatic switches that use a bimetallic, curved disk as the control element have been known to exhibit, on occasion, anomalous switching behaviors, such as a gradual drift of or sudden deviation from the original switching temperatures. A detailed analysis is presented in this report to show that a class of these switching anomalies can be attributed to an improperly designed interaction between the disk and the elastic switching

DD FORM 1473 (FACSIMILE)

UNCLASSIFIED

SECURITY CLASSIFICATION OF THIS PAGE (When Data Entered)

404 369

19. KEY WORDS (Continued)

20. ABSTRACT (Continued)

armature. The analysis is based on Wittrick's theory of thermoelastic stability of the bimetallic disk, extended to include the effects of a central force. The resulting nonlinear problem was solved numerically on a digital computer with the aid of an existing solution routine for two-point boundary-value problems. Strain energy for the various equilibrium states was calculated to investigate the stability of these states and the occurrence of the snap-through action. Numerical results indicate that under certain combinations of geometrical, mechanical and thermal conditions, the thermostat may fail to respond to temperature changes with positive snap actions of the disk, thus resulting in the so-called temperature "creepage" or "dithering" phenomenon. Such events are usually characterized by a series of openings and closings of the contacts with reduced travel but greatly increased frequency, which can induce excessive arcing or fatigue damage that would cause the thermostat to malfunction. Design formulas have been derived using an extensive parametric study; these formulas may be used to guide design improvements.

PREFACE

The author wishes to acknowledge the many valuable discussions and comments by Messrs. N. N. Au and W. M. Faust during this investigation. The assistance of Mr. J. Kane, who wrote part of the computer program and Miss M. J. McNeil, who did the drawings, is also acknowledged.

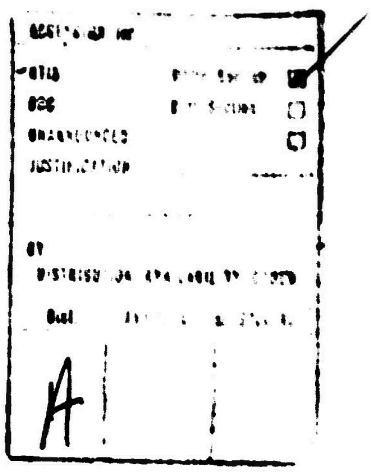

CONTENTS

FIGURES

TABLES

I. INTRODUCTION

Bimetallic disks with a small initial curvature have been used as the temperature-sensing and control element of thermostatic switches for several decades. The first detailed analysis of the thermoelastic stability of such a disk was presented in 1953 in a two-part paper[1,2]: in Part I, Wittrick[1] derived a general theory of the thermoelastic deformation of such a disk and investigated the condition for its snap-through instability; in Part II, Wittrick, Myers and Blunden[2] obtained numerical solutions to the nonlinear boundary-value problem derived in Part I with the aid of a differential analyzer (also known as an analog computer). Wittrick's analysis provided the groundwork for understanding the operation of the bimetallic-disk (BMD) thermostat by showing that, if the initial central height of the disk is greater than a critical value—approximately twice the disk thickness—the disk will respond to temperature changes with very positive snap-through actions at two fixed temperatures, one on heating and the other on cooling. This positive snap-through action is a desirable feature in tripping electric contacts since it minimizes arcing and thus prolongs the service life of the contacts.

In recent years, the BMD thermostat has attracted particularly favorable interest in the aerospace industry. The benefit of its application in a spacecraft or satellite system is obvious: the present-day BMD thermostat can be remarkably lightweight and small in size*, sealed for protection from contamination, and yet sturdy in construction for proper functioning in a shock-and-vibration environment. Furthermore, it operates solely on the thermoelastic principles and requires no external power or a gravitational field to

*A commonly used model weighs only 8.5 g (0.3 oz), measures 1.5 cm (0.6 in.) in diameter and length.

[1] Wittrick, W.H., "Stability of a Bimetallic Disk, Part I," Quart. J. Mech. Appl. Math., VI (1953), p. 15.

[2] Wittrick, W.H., D.M. Myers, and W.R. Blunden, "Stability of a Bimetallic Disk, Part II," Quart. J. Mech. Appl. Math., VI (1953), p. 26.

trip the switch (as required, respectively, by a solid-state temperature sensor or a mercury-bottle-type thermostat). All these features can qualify the miniaturized BMD thermostat as uniquely suitable for space applications if its design, manufacture and testing can be controlled to ensure the high level of reliability required in space programs. Unfortunately, the current state-of-the-art for both theoretical understanding and practical fabrication of the BMD thermostat has not yet reached such an advanced stage, partly due to the fact that since the publication of Wittrick's work[1] nearly a quarter of a century ago, very little analytical effort has been made to further the understanding of the BMD thermostat operations, as evidenced by the scarcity of applicable references in the technical literature.

It has been well-known among both manufacturers and users of the BMD thermostat that many such units can exhibit anomalous switching behaviors. One such undesirable switching anomaly is a drift in both upper and lower switching temperatures. In 1972, Henry and Coffin[3] presented a combined analytical and experimental study addressing this drift problem. Based on Wittrick's analysis, extensive numerical calculations were performed to show that high cyclic and mean stresses may develop in a typical bimetallic disk during its snapping cycles. They also compared their analytical results with strain gage measurements, obtaining reasonably good agreement. These results strongly support their proposition that high cyclic and mean stresses in the disk are the major contributing factor of the drift in its snapping temperatures during prolonged cyclic operation. As a result of their parametric study, a design procedure was proposed in Ref. 3 to limit the maximum stresses in the disk, thus alleviating the drift problem.

Recent experience of extensive applications of the miniaturized BMD thermostat in space systems has brought to light some new problems associated with its switching behavior. The most frequently encountered switching anomaly is the so-called temperature "creepage" or "dithering" phenomenon (a thermostat exhibiting such an anomaly is sometimes called a "creeper"

[3] Henry, M. F., and L. F. Coffin, Jr., "An Investigation of Switching Stresses in Bimetal Disks," Int. J. Mech. Sci., 14 (1972), p. 343.

or a "ditherer"). These terms have been used interchangeably* to describe either of the following two conditions: (1) the failure of an assembled unit to respond to temperature changes with immediate positive snap action of the disk at one of the set-temperatures during manufacturers' or users' acceptance test, or (2) a sudden deviation of the switching temperatures of a unit in service from its original set-temperatures, resulting in a very narrow switching band. The former condition usually results in high rejection rates during acceptance tests and thus in increased manufacturing cost. The latter case can be far more consequential, since such events are usually characterized by either a hesitant contact or a series of frequent openings and closings of the contacts and thus may induce excessive arcing or stress cycling; these effects often result in switch malfunction or shortened service life.

In the following sections, Wittrick's analysis[1] will be first extended to include the effects of a central force, representing the interaction between the disk and an elastic switching armature; then numerical results will be presented to show that the type of switching anomalies discussed above may be attributed to the improper regulation of such an interaction force.

---

*In this report, the two terms "creepage" and "dithering" will be used with slightly different meanings instead of interchangeably (see Section V-B for detailed discussions).

II. BIMETALLIC-DISK THERMOSTAT DESIGN AND OPERATION

There are many possible designs of a BMD thermostat, and it can be used to operate either a heat source or a heat sink to provide necessary thermal protection. For simplicity, it will be assumed that all the thermostats discussed herein are used to control an electric heater so that it is on when the contacts are closed and off when separated.

The basic designs of the BMD thermostat may be categorized into two general types, (a) and (b), as illustrated in Fig. 1. In Fig. 1(a), the contacts are closed with a built-in preload between them when the disk is disengaged from the "striker-pin," while in Fig. 1(b) the contact force is supplied by the disk-pin interaction. For applications in a space system, the type (a) design is somewhat preferable to type (b) for the following reasons:

1. Since the contact force in type (a) is preselected during design and may be calibrated during assembly, while that in type (b) is solely determined by the disk action, the latter inevitably has a higher random variance from one switch to another due to manufacturing limits of dimensional precision and material uniformity. This random variance in the contact force of type (b) switches may result in undesirable variance in their electrical characteristics and service life.

2. The elastic cantilevered armature in the type (a) design has an additional firm support at all times during its operation, i.e., either the contacts or the striker-pin (or both) are engaged, while that in type (b) has no additional firm support when the switch is in the off position. Therefore, when vibrations or dynamic transients are present, the armature in type (b) will be more susceptible to vibratory excitation that may cause accidental contact closing or arcing.

For these reasons, the following discussion and analysis will primarily concern the type (a) design; however, their extension to type (b) is straightforward.

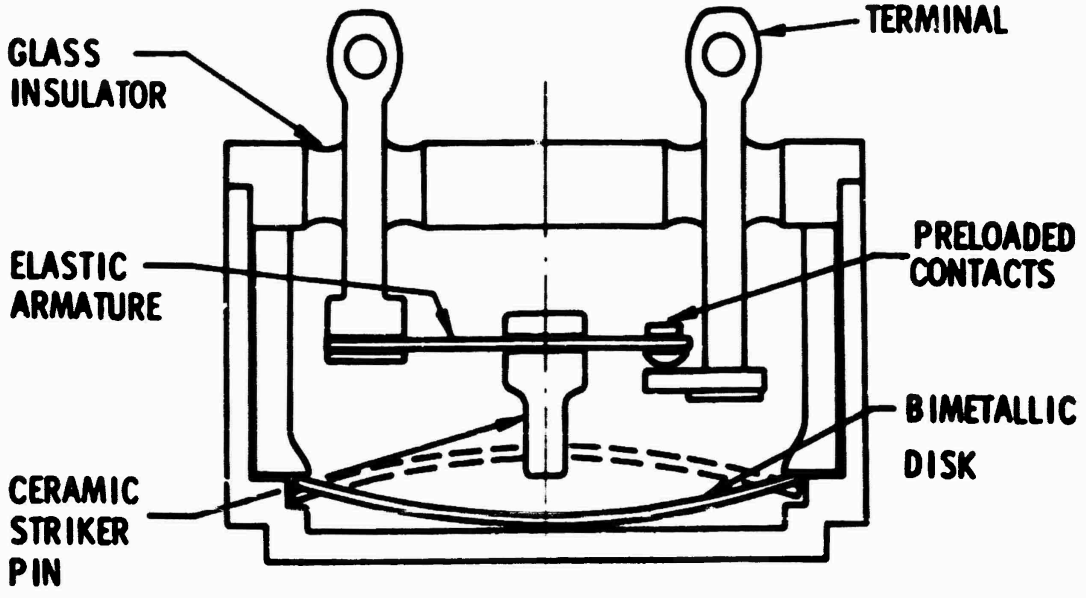

(a) Push-to-Open Design (preload between contacts)

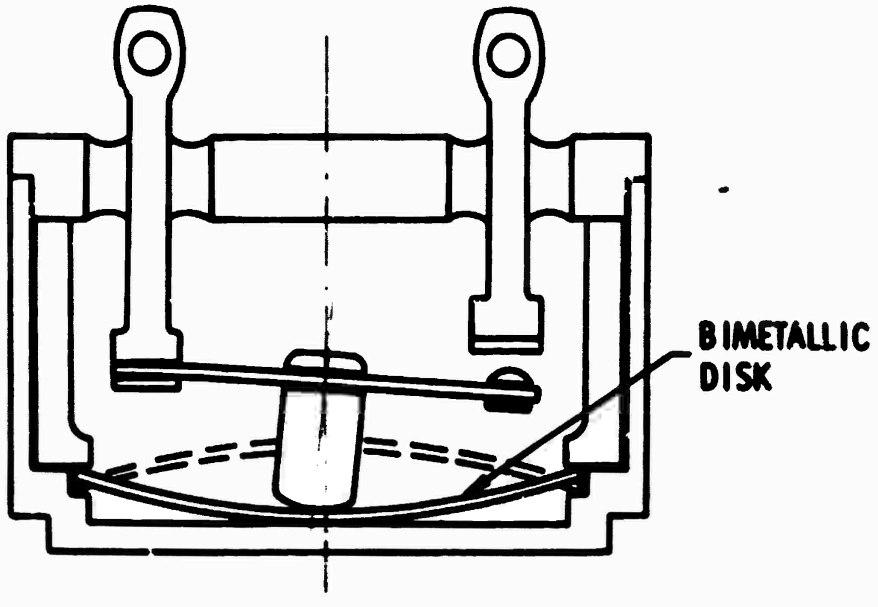

(b) Push-to-Close Design (no preload between contacts)

Fig. 1. Schematic Drawing of Bimetallic-Disk Thermostat

At this point, consider the operation of a typical BMD thermostat as shown in Fig. 1(a). For the configuration shown, the switch is on and the disk is in a "prebuckling" equilibrium state (i.e., on the same side as its stress-free state, such as points A or G in Fig. 2), with the high-expansivity metal layer on the concave side. As the disk temperature rises due to either heater output or ambient temperature rise, the disk will deform until it reaches an unstable position[1] (point B in Fig. 2) at the upper snap temperature θ_u. At this temperature, the disk snaps through toward a "postbuckling" equilibrium state (point C in Fig. 2). However, during the actual thermostat operation, the disk cannot reach the equilibrium state C as a free disk; it will first hit the striker-pin at point C_1, deform the armature until the contacts separate at point C_2, and then settle to an equilibrium state represented by point C'. Note that in order to determine this new equilibrium state C', the disk-pin interaction force must be included in the analysis. However, since this point represents the position of the system at rest, it suffices to treat this interaction as a static force (i.e., the impact and dynamic transient components of the force may be ignored).

Further examination of the nature of the armature deformation reveals that, if the disk and armature materials remain in the linear elastic range during switch operations, the disk-pin interaction force will be a bilinear function of the disk center height h, as shown in the upper part of Fig. 2. The stiffness of the armature at the striker-pin will assume a higher value k_1 between points C_1 and C_2 than the value k_2 for points beyond C_2 due to the additional support at the contact point. If the armature is very rigid with a soft rotational spring at the root, the bilinear function approaches a step function in the limit ($k_1/k_2 \to \infty$), and points C_1 and C_2 coincide. If the armature is a uniform cantilever beam with the striker-pin at the middle point, $k_1/k_2 = 32/7$. For the actual sample switches analyzed, the armature is a thin plate with a specially designed shape (sometimes plated for better conductivity), and the ratio k_1/k_2 ranges between five and seven.

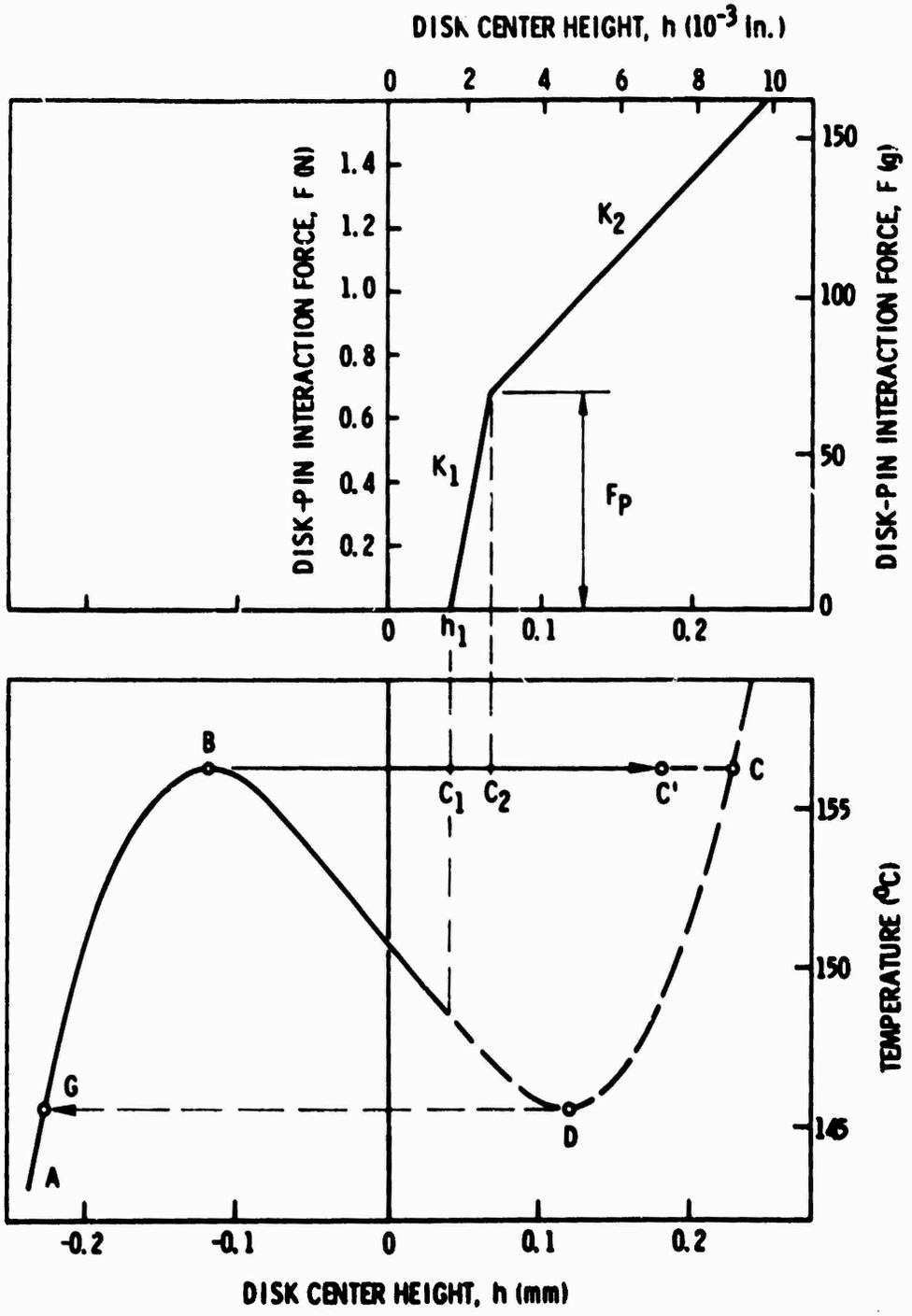

Fig. 2. Disk Snap Action and Disk-pin Interaction Force

III. ANALYSIS

Consider the bimetallic disk shown in Fig. 3. Except for the introduction of a central force F and the necessary edge support, the problem is identical to that treated in Ref. 1; the additional edge support determines an integration constant in the deflection w which differs from that in Ref. 1 only by a rigid body displacement, h_0. The notation used herein is essentially the same as that in Ref. 1 with minor modifications to conform to current prevailing notation used in shell theory (see Symbols section).

A. GOVERNING EQUATIONS FOR A DISK WITH A CENTRAL FORCE

Since the basic kinematic relations and constitutive equations for the problem under consideration are the same as Eqs. (1) through (12) of Ref. 1 and are also available in Ref. 3, they will not be repeated here. The equations of equilibrium including the central force effect are[4]

$$\frac{d}{dr}(rN_r) - N_\theta = 0 \tag{1}$$

$$rQ_r + rN_r\frac{dw}{dr} = -\frac{F}{2\pi} \tag{2}$$

$$\frac{d}{dr}(rM_r) - M_\theta - rQ_r = 0 \tag{3}$$

where w is the total distance from a point on the reference surface of the disk to the base plane (i.e., $w = w_0 + w_e$, where w_0 specifies the initial shape and w_e denotes the thermoelastic deflection), and a positive F is in the positive z direction. Note that Eq. (2) is the result of integrating the differential equation of equilibrium in the z direction, with the central force F appearing in the integration constant.

[4] Reissner, E., "Symmetric Bending of Shallow Shells of Revolution," J. Math. & Mech., 7 (1958), p. 121.

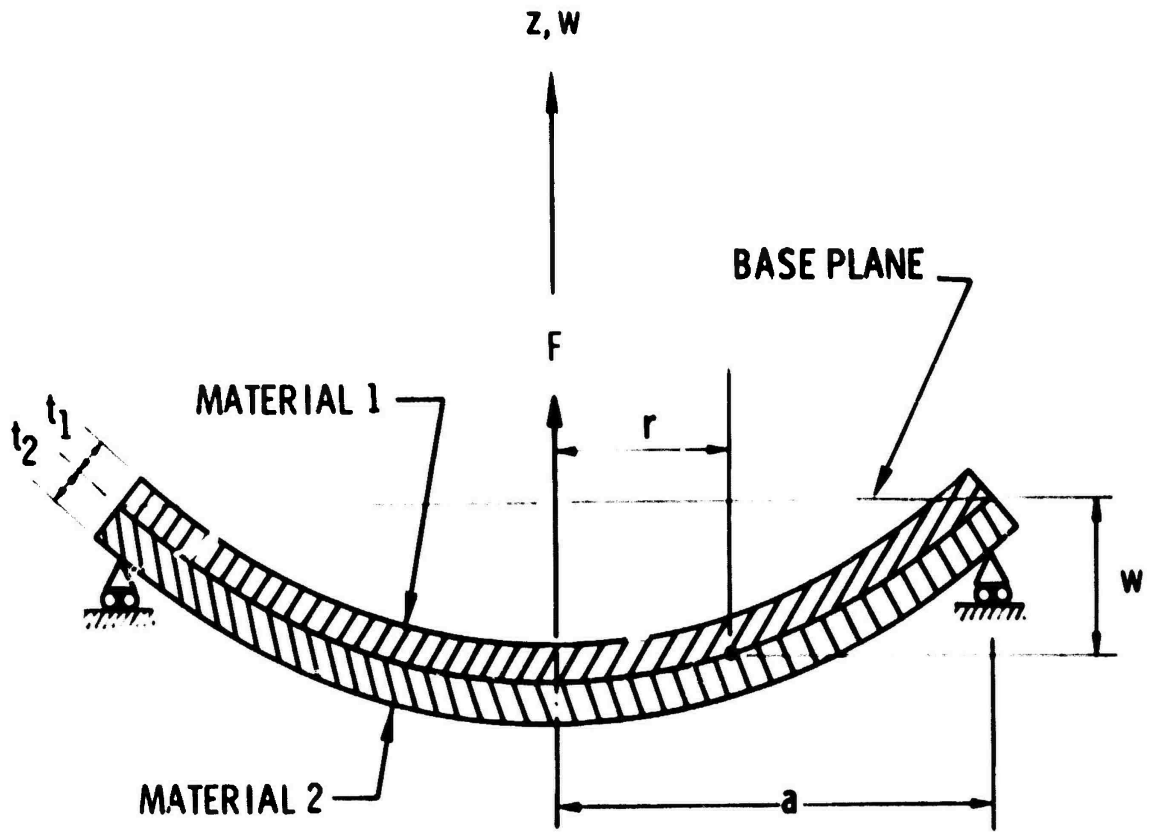

Fig. 3. Geometry and Coordinate Convention for Bimetallic Disk

Upon elimination of the shear stress resultant Q_r, Eqs. (2) and (3) combine to give

$$\frac{d}{dr}(rM_r) - M_\theta + rN_r\frac{dw}{dr} = -\frac{F}{2\pi} \tag{4}$$

Equation (1) is the same as Eq. (14) of Ref. 1, while Eq. (4) differs from Eq. (15) thereof only by the additional term $F/2\pi$.

Denote the elastic rotation of a normal to the disk as a new variable β; then, within the scope of a thin shell theory

$$\beta = \frac{dw_e}{dr} = \frac{dw}{dr} - \beta_o \tag{5}$$

where $\beta_o = dw_o/dr$. The equivalent flexural rigidity D^* and the equivalent Poisson's ratios ν_B, ν_C, and ν_D are now defined as follows:

$$D^* = D - \frac{C^2}{B}; \qquad \nu_D = \frac{1}{D^*}\left(D' - \frac{CC'}{B}\right);$$

$$\nu_B = \frac{B'}{B}; \qquad \nu_C = \frac{C'}{C};$$

where the quantities B, C, D, B', C', and D' are the same as in Ref. 1. The same elimination procedure used in Ref. 1 reduces the basic set of equations to the following two coupled differential equations [cf., Eqs. (16) and (17) of Ref. 1]:

$$\frac{1}{r}\frac{d}{dr}\left(r^3\frac{dN_r}{dr}\right) + (\nu_C - \nu_B)Cr\frac{d}{dr}\left[\frac{1}{r}\frac{d}{dr}(r\beta)\right] + (1-\nu_B^2)B\left(\beta_o\beta + \frac{1}{2}\beta^2\right) = 0 \tag{6}$$

$$r\frac{d}{dr}\left[\frac{1}{r}\frac{d}{dr}(r\beta)\right] - \frac{r}{D^*}N_r(\beta_o + \beta) = -\frac{F}{2\pi D^*} \tag{7}$$

The two boundary conditions at the disk edge are the same as that in Ref. 1; i.e.,

$$N_r = 0 \quad \text{at } r = a \tag{8}$$

and

$$\frac{d\beta}{dr} + \nu_D \frac{\beta}{r} = - \frac{Q^*}{D^*} \theta \quad \text{at } r = a \tag{9}$$

where θ is the disk temperature measured from a reference temperature at its stress-free state, and

$$Q^* = Q - \frac{PC}{B}$$

in which Q and P are also defined in Ref. 1. The other two boundary conditions at the disk center must be modified to account for the singularity introduced by the central force F. If F is assumed to be small, so that it causes only a linear perturbation of the thermoelastic deformation, the linear singular solution for such a shallow shell, similar to those given in Refs. 5 through 8, applies:

$$\lim_{r \to 0} N_r = \frac{F}{4\pi D^*} (\nu_C - \nu_B) C \lim_{r \to 0} \ln\left(\frac{r}{a}\right) + \text{finite terms} \tag{10}$$

$$\lim_{r \to 0} \beta = \frac{F}{4\pi D^*} \lim_{r \to 0} \left[r \ln\left(\frac{r}{a}\right) \right] \tag{11}$$

---

[5] Reissner, E., "Stresses and Small Displacements of Shallow Spherical Shells, Part I," J. Math. & Phys., 25 (1947), p. 80.

[6] Reissner, E., "Stresses and Small Displacements of Shallow Spherical Shells, Part II," J. Math. & Phys., 25 (1947), p. 279.

[7] Flügge, W., and R. Elling, "Singular Solutions for Shallow Shells," Int. J. Solids & Struc., 8 (1972), p. 227.

[8] Simmonds, J.G., and M.R. Bradley, "The Fundamental Solutions for a Shallow Shell with an Arbitrary Quadratic Midsurface," J. Appl. Mech., 43 (Trans. ASME, 92, Series E) (1976), p. 286.

These relationships will be useful in obtaining numerical solutions to the problem.

It should be noted that the bending moments M_r and M_θ, which are dependent on the changes in curvatures $d\beta/dr$ and (β/r), are always singular under the force F, but the membrane forces N_r and N_θ are singular only when the quantity $(\nu_C - \nu_B)C$ is nonzero. When the Poisson's ratios of the two metal layers are equal (i.e., $\nu_1 = \nu_2$, as assumed in the latter part of Ref. 1), the quantity $(\nu_C - \nu_B)$ in Eq. (10) above vanishes, and the stress resultant N_r becomes finite under the force F, as in a single-layered shallow spherical shell.[7] But if ν_1 and ν_2 are slightly different (say, $\nu_1 = 0.30$ and $\nu_2 = 0.29$, as used in the numerical examples below), N_r contains a singularity under the force F. This phenomenon is somewhat similar to the effect of a slight deviation of the shell geometry from perfectly spherical (i.e., slightly ellipsoidal); in this case, a singular term proportional to the difference of the two principal curvatures exists in N_r as shown by Flügge and Elling.[7]

This rather strong effect of the condition $\nu_1 = \nu_2$ on the membrane-stress singularity raises a question of both theoretical and practical significance: Are the conclusions drawn from Wittrick's analysis[1] (in which the above condition was used) concerning the thermoelastic stability of the bimetallic curved disk strongly dependent on that condition? It is shown below that, when the condition $\nu_1 = \nu_2$ is relaxed, all the major conclusions arrived at in Ref. 1 are still valid, except that the symmetry property of the solutions [see Eq. (33) of Ref. 1] no longer holds exactly.

B. FREE DISK INITIALLY IN THE FORM OF A SHALLOW SPHERICAL CAP

When the initial form of the disk is a shallow spherical shell, its initial reference surface may be approximated by

$$w_o = h_o\left(\frac{r^2}{a^2} - 1\right). \tag{12}$$

This gives $\beta_o = 2h_o r/a^2$. In the absence of the central force F, it may be readily shown by direct substitution that the following three particular solutions satisfy Eqs. (6) and (7) and all boundary conditions exactly.

Solution (a), Stress-free State:

$$\beta = 0 \text{ and } N_r = 0, \text{ when } \theta = 0$$

Solution (b), Flat State:

$$\beta = -\beta_o \text{ and } N_r = N_{rm}\left(1 - \frac{r^2}{a^2}\right), \text{ when } \theta = \theta_m$$

Solution (c), Reversed State:

$$\beta = -2\beta_o \text{ and } N_r = 0, \text{ when } \theta = 2\theta_m$$

In the above solutions, θ_m is the "mean temperature" discussed in Ref. 1, and may be obtained by substituting $\beta = -\beta_o$ in Eq. (9). Thus

$$\theta_m = \frac{(1+\nu_D)D^*}{Q^*}\left(\frac{2h_o}{a^2}\right) \tag{13}$$

The term N_{rm} is the maximum compressive stress-resultant at the disk center when the disk is flat [cf., Eq. (34) of Ref. 1]; it may be obtained by substituting $\beta = -\beta_o$ into Eq. (6), integrating the resulting equation and determining the integration constant by Eq. (8). Thus

$$N_{rm} = -\frac{1}{4}\left(1 - \nu_B^2\right)B\left(\frac{h_o}{a}\right)^2. \tag{14}$$

The above three particular solutions for a free disk are essentially the same as those discussed in detail in Ref. 1, except that Eqs. (13) and (14) are now also valid for the more general case, $\nu_1 \neq \nu_2$. When ν_1 and ν_2 are set equal, Eq. (14) agrees with Eq. (34) of Ref. 1, but an attempt to reduce Eq. (13)

above to Eq. (46) of Ref. 1 will reveal that the coefficient K of the latter equation, as given by Eq. (47) thereof, contains an extraneous factor $(1 + \nu)$, which is believed to be an algebraic error. This error invalidates the calculated values of K in Table 3 of Ref. 1, but does not affect the analysis of Refs. 1 through 3 in any other way.

Consider next the symmetry property of the solutions with respect to the particular solution (b) above (i.e., the flat position of the disk) as discussed in Eq. (33) of Ref. 1. Specifically, if

$$\beta = -\beta_o + \bar{\beta} \text{ and } N_r = \bar{N}_r, \text{ when } \theta = \theta_m - \bar{\theta}$$

is a solution to the free disk problem, examination is required as to whether the following is also a solution:

$$\beta = -\beta_o - \bar{\beta} \text{ and } N_r = \bar{N}_r, \text{ when } \theta = \theta_m + \bar{\theta} . \qquad (15)$$

Direct substitution of Eq. (15) into Eq. (6) indicates that Eq. (6) is not satisfied, owing to the presence of its second term. Therefore, this symmetry property of the solutions no longer holds exactly if $\nu_1 \neq \nu_2$, although it may be expected to hold approximately if ν_1 and ν_2 are close.

Finally, it is necessary to reexamine the critical initial height of the disk h_{cr}, which is the minimum value of h_o for the thermal snap action to occur. A detailed examination of Wittrick's procedure[1] for determining h_{cr} shows that the procedure will remain valid for the more general case of unequal Poisson's ratio if the following generalized definitions of the parameters λ and ϕ_o are used in place of Eqs. (28) and (30) of Ref. 1:

$$\lambda = \frac{a^2 Q^*}{(1 + \nu_D) D^*} \left[\frac{(1 - \nu_B^2) B}{2D^*} \right]^{1/2} \qquad (16)$$

$$\phi_o = 2h_o \left[\frac{(1 - \nu_B^2) B}{2D^*} \right]^{1/2} \qquad (17)$$

Note that the Poisson's ratio in Eqs. (31), (38) and (42) of Ref. 1 must also be changed to ν_D, as seen from Eq. (23) thereof. With these minor changes, the critical values of ϕ_o may be calculated for a given value of ν_D through the same procedure described in Ref. 1. This calculation has been performed for various values of ν_D, and the results are listed in Table 1 for reference.

Table 1. Critical Values of ϕ_o

ν_D	0.0	0.1	0.2	0.3	0.4	0.5
ϕ_{cr}	8.1590	8.4186	8.6537	8.8674	9.0627	9.2417

If an "equivalent thickness" of the disk is defined as

$$t_{eq} = (12\, D^*/B)^{1/2} \tag{18}$$

then, from Eq. (17), it is seen that thermal snap action of the disk will occur if

$$h_o > \frac{\phi_{cr}\, t_{eq}}{\sqrt{24\left(1 - \nu_B^2\right)}} \tag{19}$$

Condition (19) above reduces to Condition (44) of Ref. 1 when $\nu_1 = \nu_2$.

From the above discussion, it may be concluded that when the curved disk is made of two material layers with unequal Poisson's ratios, its thermoelastic snap behavior remains essentially the same as described in Ref. 1.

When a central force is present on the disk, however, no simple, closed-form particular solutions can be found similar to those found for a free disk. Furthermore, the problem is no longer tractable by following the power-series solution procedure successfully employed in Ref. 2. Therefore, a direct numerical solution was pursued in the following analysis.

IV. NUMERICAL SOLUTIONS

The common numerical techniques for solving two-point boundary-value problems can be classified as either "finite-difference" or "shooting"[9] methods. For a nonlinear problem, such as the present one, finite-difference methods will result in a large system of nonlinear algebraic equations, thus losing much of their attractiveness because of the difficulty in itself of solving a large nonlinear algebraic system on a digital computer. The shooting method is a procedure in which the differential equations are numerically integrated as an initial value problem with estimated unknown initial values, and the boundary conditions at the far end are satisfied by iterative corrections of these initial estimates. In the following discussion, numerical solutions will be obtained with the aid of an existing FORTRAN IV code developed by Gold[10], which is based on an improved shooting technique due to Morrison, Riley and Zancanaro.[9]

In order to use the shooting method, the two-point boundary value problem is restated in the following form as a system of four first-order differential equations

$$\frac{d\beta}{dr} = -\kappa_r \tag{20a}$$

$$\frac{du}{dr} = \epsilon_r - \frac{2h_o r}{a^2}\beta - \frac{1}{2}\beta^2 \tag{20b}$$

$$\frac{dN_r}{dr} = \frac{N_\theta - N_r}{r} \tag{20c}$$

$$\frac{dM_r}{dr} = \frac{M_\theta - M_r}{r} - \left(\frac{2h_o r}{a^2} + \beta\right)N_r + \frac{F_o}{2\pi r} \tag{20d}$$

---

[9] Morrison, D. D., J. D. Riley, and J. F. Zancanaro, "Multiple Shooting Method for Two-Point Boundary Value Problems," Communications of the Assoc. for Computing Machinery, 5 (1962), p. 613.

[10] Gold, Barbara J., "Subroutine TPBV," The Aerospace Corporation, Mathematics and Computation Center Library (1968).

where κ_r is the change in meridional curvature, ϵ_r is the meridional membrane strain, and N_θ, M_θ, respectively, are the stress- and couple-resultants in the circumferential direction. These four auxiliary variables are related to the four primary variables β, u, N_r and M_r by the following algebraic equations:

$$\begin{aligned}
\kappa_r &= \frac{1}{D^*}\left[M_r - \frac{C}{B}N_r + Q^*\theta\right] + \nu_D\frac{\beta}{r} \\
\epsilon_r &= \frac{1}{B}\left[N_r - C\left(\kappa_r - \nu_C\frac{\beta}{r}\right) + P\theta\right] - \nu_B\frac{u}{r} \\
N_\theta &= B\left(\frac{u}{r} + \nu_B\epsilon_r\right) - C\left(\frac{\beta}{r} - \nu_C\kappa_r\right) - P\theta \\
M_\theta &= \frac{C}{B}N_\theta - D^*\left(\frac{\beta}{r} - \nu_D\kappa_r\right) - Q^*\theta
\end{aligned} \tag{21}$$

The boundary conditions at the disk center are

$$\beta(0) = 0; \qquad u(0) = 0. \tag{22}$$

Those at the edge, r = a, are

$$N_r(a) = 0; \qquad M_r(a) = 0. \tag{23}$$

Note that a constant force $F = -F_o$, which appears in Eq. (20d), has been assumed. Methods of treating a variable force will be described in Section V-A.

In order to circumvent the numerical problem associated with the singularity at r = 0, it is assumed that the striker-pin has a small but finite radius $r = R_{pin}$, and that the force F_o is produced by a uniformly distributed pressure within the small region $r \leq R_{pin}$. Since the solutions are now finite, the condition of axial symmetry gives

$$N_r = N_\theta, \text{ and } M_r = M_\theta \text{ (for } r \to 0). \tag{24}$$

By combining the above conditions with Eqs. (21), it can be easily shown that

$$\frac{\beta}{r} = -\kappa_r, \text{ and } \frac{u}{r} = \epsilon_r \text{ (for } r \to 0). \tag{25}$$

With the aid of Eqs. (24) and (25), the singularity in Eqs. (20) and (21) can be removed. Thus, Eqs. (20c) and (20d) are replaced by

$$\left.\begin{aligned} \frac{dN_r}{dr} &= 0 && (20c') \\ \frac{dM_r}{dr} &= -\left(\frac{2h_o r}{a^2} + \beta\right) - \frac{F_o r}{2\pi R_{pin}^2} && (20d') \end{aligned}\right\} \text{(for } r \to 0)$$

and Eqs. (21) are replaced by

$$\left.\begin{aligned} \kappa_r &= \frac{1}{(1+\nu_D)D^*}\left[M_r - \frac{C}{B}N_r + Q^*\theta\right] \\ \epsilon_r &= \frac{1}{(1+\nu_B)B}\left[N_r - (1+\nu_C)C\kappa_r + P\theta\right] \\ N_\theta &= (1+\nu_B)B\,\epsilon_r + (1+\nu_C)C\kappa_r + P\theta \\ M_\theta &= \frac{C}{B}N_\theta + (1+\nu_D)D^*\kappa_r - Q^*\theta \end{aligned}\right\} \text{(for } r \to 0) \tag{21'}$$

From extensive numerical results, it was found that as long as $R_{pin} \ll a$, the solutions are independent of the assumed values of R_{pin}—as far as the disk center height h and the snapping temperatures θ_u and θ_ℓ are concerned. However, the local bending moments M_r and M_θ were found to increase slowly with decreasing R_{pin} values.

A. ESTIMATES OF THE UNKNOWN INITIAL VALUES

The key factor in an efficient application of the shooting method is to provide reasonably close estimates of the unknown initial values, in this case $N_r(0)$ and $M_r(0)$. If a given temperature θ_1 is sufficiently below the snapping temperatures [say, $\theta_1 \leq (1/2)\theta_m$], the following estimates are close enough to yield solutions (accuracy requirement: four significant digits) within eight iterations.

$$N_r(0) \approx N_{rm}\left(1 - \sqrt{1 - \theta_1/\theta_m}\right) - (\nu_C - \nu_B)C\left(\frac{F_o}{4\pi D^*}\right)\ln(R_{pin}/a) \qquad (26)$$

$$M_r(0) \approx \frac{(2 + \nu_D)h_o}{6} N_{rm}\left(1 - \sqrt{1 - \theta_1/\theta_m}\right) - (1 + \nu_D)\left(\frac{F_o}{4\pi}\right)\ln(R_{pin}/a) \qquad (27)$$

Note that the first terms of Eqs. (26) and (27) are obtained empirically by assuming that the stress-resultant N_r increases with the temperature θ in a parabolic form, while the second terms thereof were obtained from the singular solutions, Eqs. (10) and (11).

When final solutions at two selected temperatures θ_1 and θ_2 have been obtained using the above initial estimates, subsequent solutions for higher temperatures may start with better estimates of the unknown initial values by using linear extrapolation. A sequence of solutions may then be obtained at a preselected temperature increment $\Delta\theta$ until no convergence can be reached. This will indicate that the upper snapping temperature θ_u has been exceeded. At this point, $\Delta\theta$ is reduced by a factor of ten, and the solution is carried forward from the last convergent temperature. This procedure is repeated until the upper snapping temperature θ_u is determined to the desired accuracy. The lower snapping temperature θ_l is determined in a similar manner with a temperature decrement $-\Delta\theta$. A computer code has been developed to carry out the above procedures automatically.

B. STRAIN ENERGY CALCULATIONS

In order to investigate the stability of the various equilibrium positions, the strain energy in the disk is calculated for each convergent solution. Let δU denote the strain energy density per unit area of the reference surface; then

$$\delta U = \frac{1}{2} \int_{-t_2}^{t_1} (\sigma_r e'_r + \sigma_\theta e'_\theta) d\zeta \tag{28}$$

where ζ is the thickness coordinate measured from the bond surface of the two layers. The elastic strains e'_r and e'_θ are given by the relationships

$$\begin{aligned} e'_r &= e_r - \alpha_i \theta = (\epsilon_r - \alpha_i \theta) + \zeta \kappa_r \\ e'_\theta &= e_\theta - \alpha_i \theta = (\epsilon_\theta - \alpha_i \theta) + \zeta \kappa_\theta \end{aligned} \tag{29}$$

Note that α_i assumes the value α_1 for $\zeta > 0$, and α_2 for $\zeta < 0$. The quantities $\epsilon_\theta = u/r$ and $\kappa_\theta = -\beta/r$ are, respectively, the membrane strain and curvature change in the hoop direction. Substituting Eqs. (29) into (28) and integrating the result, one obtains

$$\begin{aligned} \delta U = {} & \frac{1}{2}[N_r \epsilon_r + N_\theta \epsilon_\theta + M_r \kappa_r + M_\theta \kappa_\theta] \\ & - \frac{1}{2} \alpha_2 \theta \int_{-t_2}^{0} (\sigma_r + \sigma_\theta) d\zeta - \frac{1}{2} \alpha_1 \theta \int_{0}^{t_1} (\sigma_r + \sigma_\theta) d\zeta \end{aligned} \tag{30}$$

Finally, the stresses σ_r and σ_θ can be expressed in terms of the membrane strains ϵ_r and ϵ_θ and curvature changes κ_r and κ_θ [cf., Eqs. (4) of Ref. 1]. Equation (30) can thus be simplified to read as follows:

$$\delta U = \frac{1}{2}\left[N_r\epsilon_r + N_\theta\epsilon_\theta + M_r\kappa_r + M_\theta\kappa_\theta\right] + P_2\theta^2 - \frac{1}{2}P\theta(\epsilon_r + \epsilon_\theta) - \frac{1}{2}Q\theta(\kappa_r + \kappa_\theta) \tag{31}$$

where

$$P_2 = \frac{E_1\alpha_1^2 t_1}{1 - \nu_1} + \frac{E_2\alpha_2^2 t_2}{1 - \nu_2} . \tag{32}$$

Integration of the above expression for δU over the entire reference surface gives the total strain energy in the disk

$$U_d = \int_0^a \int_0^{2\pi} \delta U \, r d\theta dr = 2\pi \int_0^a \delta U \, r dr \tag{33}$$

Note that the work done by the force F, which gives the strain energy increase in the armature from the preload state, must be added to U_d to obtain the total strain energy of the disk-armature system. That is

$$U_{total} = U_d + \int_{h_1}^{h_e} F(h)\, dh \tag{34}$$

where h_1 and h_e are the disk center height at the striker-pin engagement position and at the equilibrium state under consideration, respectively.

For a given equilibrium state at a specified temperature, the total strain energy calculated from Eq. (34) must be a stationary value with respect to a virtual displacement δh (corresponding to an admissible change of disk shape δw); it may be a minimum, a maximum, or a point of inflection. The equilibrium state is stable only when the total strain energy is a local minimum. If the strain energy is a local maximum, the disk is in unstable equilibrium, and it will snap to one of two possible stable equilibrium positions, having lower total strain energy. If the strain energy is at an inflection point, the disk is again at unstable equilibrium, and it will snap to a unique stable equilibrium position (see Fig. 5 for additional clarification of these three types of equilibrium positions).

V. NORMAL AND ANOMALOUS SWITCHING CYCLES

In order to investigate the switching behavior of the type (a) BMD thermostats, a detailed numerical analysis was performed on a typical BMD thermostat design which has been used extensively in recent space programs and has experienced dithering problems. Its parameters, physical and calculated, and certain performance specifications are shown in Table 2. Although the nominal switching band of the particular batch of thermostats being analyzed is listed as 5.6°C (10°F), it is interesting to note that the specification gives the switching band as 1.1°C-9.0°C (2°F-16°F), an indication of wide unit-to-unit variations.

As discussed in Ref. 3, the bimetallic disks used in these thermostats are formed by a series of stamping operations, with only incomplete stress relief; consequently, the end product undoubtedly contains high residual stresses at room temperature. One evidence of the presence of these residual stresses in the disks is the subcritical disk center height at room temperature. The stress-free state[1], even if one assumes it can be recovered by a temperature change alone, is at an unknown temperature, which cannot be measured directly.

In the following applications of the theory, the "inverse" procedure first used in Ref. 3 is employed to determine the initial disk center height h_o; i.e., a series of trial values of h_o is used in the analysis until the calculated snapping temperature band $\Delta\theta \equiv \theta_u - \theta_\ell$ matches the measured band for a free disk, $\Delta T \equiv T_u - T_\ell$ (note that the latter is, in general, different from the thermostat switching band $\Delta T'$, as will be discussed in more detail in the next section).

The rationale for this procedure is based on the fact that the residual stresses in the bimetallic disk must satisfy the same set of shell equations and boundary conditions as do the thermal stresses caused by a temperature rise. Whereas the thermal stresses are caused by unequal thermal expansions in the two layers [i.e., the $P\theta$ and $Q^*\theta$ terms in Eqs. (9) through (12) of Ref. 1], the residual stresses are primarily caused by the unloading of the

Table 2. Thermostat Parameters

a. Disk Physical Parameters	
Thermal expansion coefficient	$\alpha_1 = 26.3 \times 10^{-6}\ ^{o}C^{-1}$ $(14.6 \times 10^{-6}\ ^{o}F^{-1})$ $\alpha_2 = 2.2 \times 10^{-6}\ ^{o}C^{-1}$ $(1.2 \times 10^{-6}\ ^{o}F^{-1})$
Young's Modulus	$E_1 = 124.1$ GPa $(18.0 \times 10^{6}$ psi) $E_2 = 156.5$ GPa $(22.7 \times 10^{6}$ psi)
Poisson's Ratio	$\nu_1 = 0.30$ $\nu_2 = 0.29$
Thickness	$t_1 = 0.12$ mm (0.0047 in.) $t_2 = 0.11$ mm (0.0043 in.)
Disk Radius	$a = 6.35$ mm (0.25 in.)
Disk center height at RT	$h_{RT} = 0.3$ mm (0.012 in.)
b. Performance Specifications	
Upper switching temperature	$T_u = 51.7 \pm 1.7^{o}C$ $(125 \pm 3^{o}F)$
Lower switching temperature	$T_l' = 46.1\ ^{+2.8}_{-1.7}\ ^{o}C$ $(115\ ^{+5}_{-3}\ ^{o}F)$
Switching band	$\Delta T' = 1.1^{o}C - 9.0^{o}C$ $(2^{o}F - 16^{o}F)$
Striker-pin force required to overcome contact preload	$F_p = 0.68$ N
c. Calculated Parameters	
Critical value of h_o	$h_{cr} = 0.435$ mm (0.01714 in.)
Disk center height at "stress-free" state	$h_o = 0.48$ mm (0.0189 in.)
Mean temperature of disk snap points	$\theta_m = 150.8$ (^{o}C from reference temperature)
Upper snap point	$\theta_u = 156.2$ (^{o}C from reference temperature)
Equivalent Poisson's ratios	$\nu_B = 0.295$, $\nu_C = 0.0912$, $\nu_D = 0.295$
Spring constants of armature at striker-pin*	$k_1 = 26$ N/mm, $k_2 = 5$ N/mm

*Calculated from a finite-element plate analysis and verified by lab measurements

unequal yield stresses in the two metal layers at the end of the forming process. Therefore, within the scope of a thin shallow shell theory, it is not unreasonable to expect that this residual stress state may be approximated by a thermal stress state to the extent that their effects on such gross structural behavior as snap buckling or free vibration would be equivalent.

Application of the above procedure indicates that, for the thermostat discussed herein, the disk snapping band of $\Delta\Theta = 10.8^{o}C$ corresponds to the initial center height $h_o = 0.48$ mm, and that the "equivalent stress-free state" is at the reference temperature $T_o = -104.5^{o}C$.

A. NORMAL THERMOSTAT

The effects of a central force on the thermoelastic deformation of the disk is shown in Fig. 4, in which a family of curves, corresponding to a set of constant forces ($F_o = 0.5\ F_p,\ F_p,\ \ldots,\ 2.5\ F_p$) is plotted, together with the baseline curve for the free disk ($F_o = 0$). These S-shaped curves show the disk center height h of the equilibrium configuration as a function of the disk temperature Θ. An interesting observation from Fig. 4 is the striking similarity of all these curves. Within the accuracy of the numerical results, it was found that each of these curves is congruent to the baseline curve and is at a temperature shift $\delta\Theta$ from this curve. The shift $\delta\Theta$ was found empirically to be proportional to the magnitude of the force F_o; i.e.,

$$\delta\Theta = 0.130\ (F_o/Q^*), \tag{35}$$

The above result indicates that the snap band $\Delta\Theta$, the two values of disk center height at which instability occurs, and the throw of the disk during snap-through are not affected by the presence of the stresses due to a constant central force F_o. This feature provides further support to the inverse procedure used previously in the treatment of the unknown residual stress condition, since it shows that the snapping characteristics of the disk are not sensitive to the detailed prestress distribution therein.

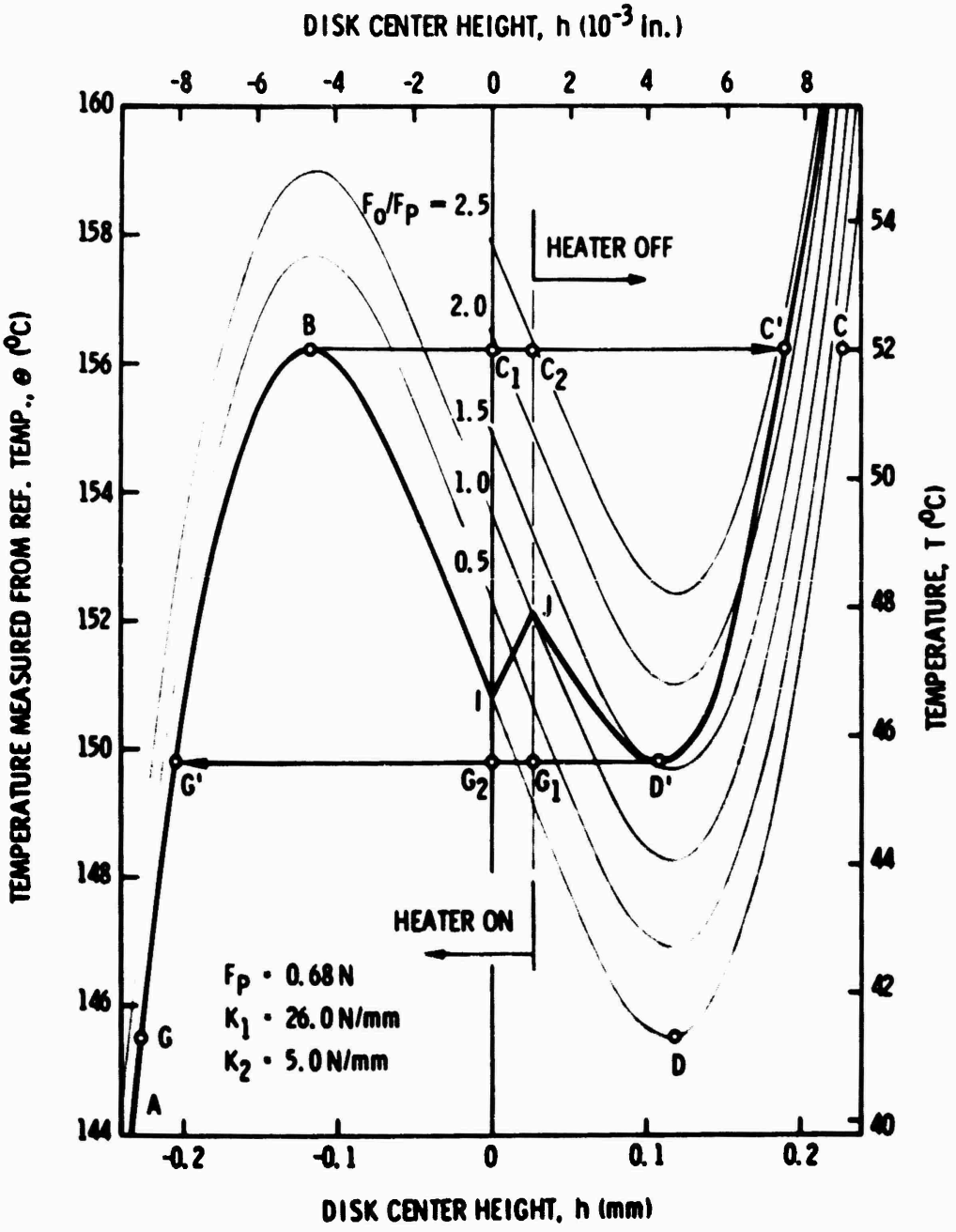

Fig. 4. Disk Center Height versus Temperature—Normal Switch (switching cycle ABC'D'G')

The above family of h-θ curves (for different F_o values), combined with a family of vertical straight lines, provides a network of curvilinear coordinates for tracing equilibrium states of a disk with a variable striker-pin force F = F(h). If the striker-pin is assumed to engage the disk at its flat position (i.e., $h_1 = 0$), and the force function is bilinear as illustrated in Fig. 2, the h-θ curve corresponds to the heavy line ABIJD'C' in Fig. 4. Note that this curve no longer has a simple S-shape, but has abrupt slope changes at both the point of striker-pin engagement I and that of contact separation J. It is important to point out that the loop G'BC'D'G' represents a normal thermostat switching cycle. In this cycle, the upper snap point B remains the same as that of the free disk, but the lower snap point D' is different from point D of the free disk. It is apparent that the lower snap temperature may be raised significantly by the interaction force F; consequently, the snap band for the switch $\Delta\theta'$ may be considerably less than $\Delta\theta$, the free-disk snap band. However, the disk center height at which the lower snap action occurs appears to be only slightly affected by the force F.

The total strain energy of the disk-armature system, as well as that of the free disk, are illustrated in Fig. 5 for selected temperatures. It is worthy of note that in the neighborhood of the lower snap point D', the total strain energy decreases only slightly as the disk center moves toward the contact closing point G_1, an indication that the lower snap action of this thermostat may start with an undesirable, slow motion; such motion could give rise to hesitant contact closure.

B. ANOMALOUS THERMOSTATS

It is apparent from an inspection of Fig. 4 that the position of striker-pin engagement, or h_1, must be kept within a very tight tolerance for the thermostat to function properly. For the thermostat under consideration, this allowable tolerance is on the order of 0.1 mm (0.004 in.). Since control of manufacturing tolerances to this level is difficult, if not impractical, it is not surprising that high rejection rates in acceptance tests and persistent problems during service were experienced with this thermostat.

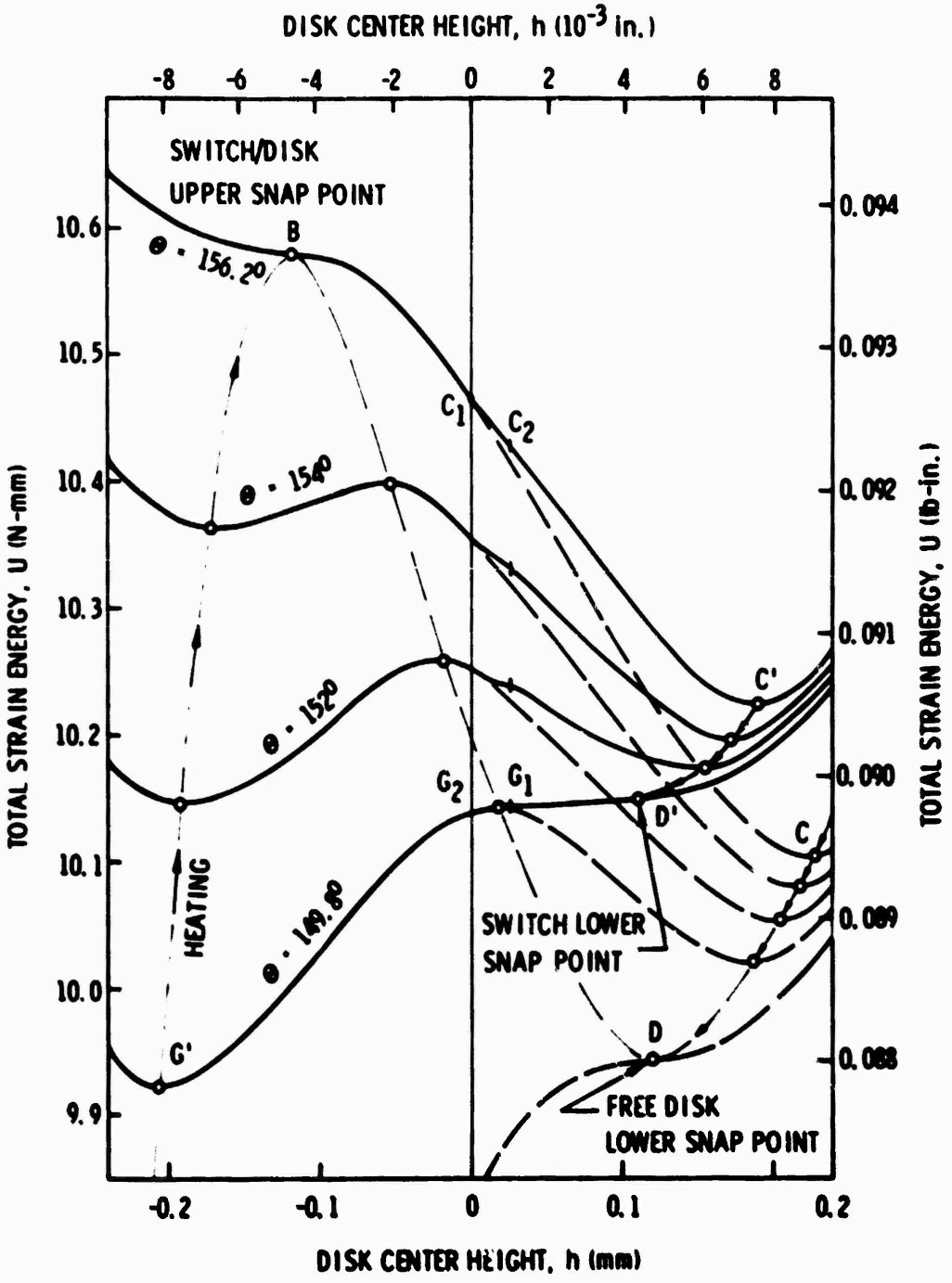

Fig. 5. Strain Energy in Free Disk (dashed lines) and in Disk-Armature System (solid lines)—Normal Switch (see Fig. 4)

First, consider the thermostat in which the striker-pin is too long, so that at the upper snap temperature it engages the disk before the latter snaps past the flat position. In such a case, the drop in strain energy from the upper snap point B to the contact-opening point C_2 (see Fig. 5) is relatively small. This available energy may be insufficient to overcome the barrier of electric potential, and the contacts may fail to open immediately. Although further temperature rise will increase the disk-pin interaction force and eventually open the contacts, this delay in contact opening is undesirable because it will leave the contacts momentarily in a condition of poor contact, thus susceptible to arcing.

Consider next the thermostat in which the striker-pin is too short, so that at the lower snap temperature the contacts close before the disk is set in motion (see Fig. 6). In such a case, the disk-armature system is in a stable condition when the contacts are in a threshold contact; consequently, the contacts will alternatively open and close with thermally induced motion instead of snap action. This anomalous form of switching will be referred to in this report as "creepage".

It should be pointed out that the above anomaly may escape detection in a functional test in which the temperature changes are controlled independently of the electrical contacts (such as by a liquid bath, a commonly used method), since the disk temperature θ would then continue to decrease after contact closing. When the temperature reaches point I (Fig. 6), the disk disengages from the striker-pin and snaps to the prebuckling configuration G'. However, if a sufficiently slow rate of change of the disk temperature is maintained in such a test, a time lapse should be easily detected between the contact closing (which may be recorded as an electric signal) and the disk snapping (an acoustic or accelerometer signal).

If the thermostat is used to control power to a heater upon which the thermostat is mounted, and its disk-pin engagement point I is made slightly closer to the base-plane of the disk than in the previous case (as shown in Fig. 7), a more complex and interesting switching anomaly may result.

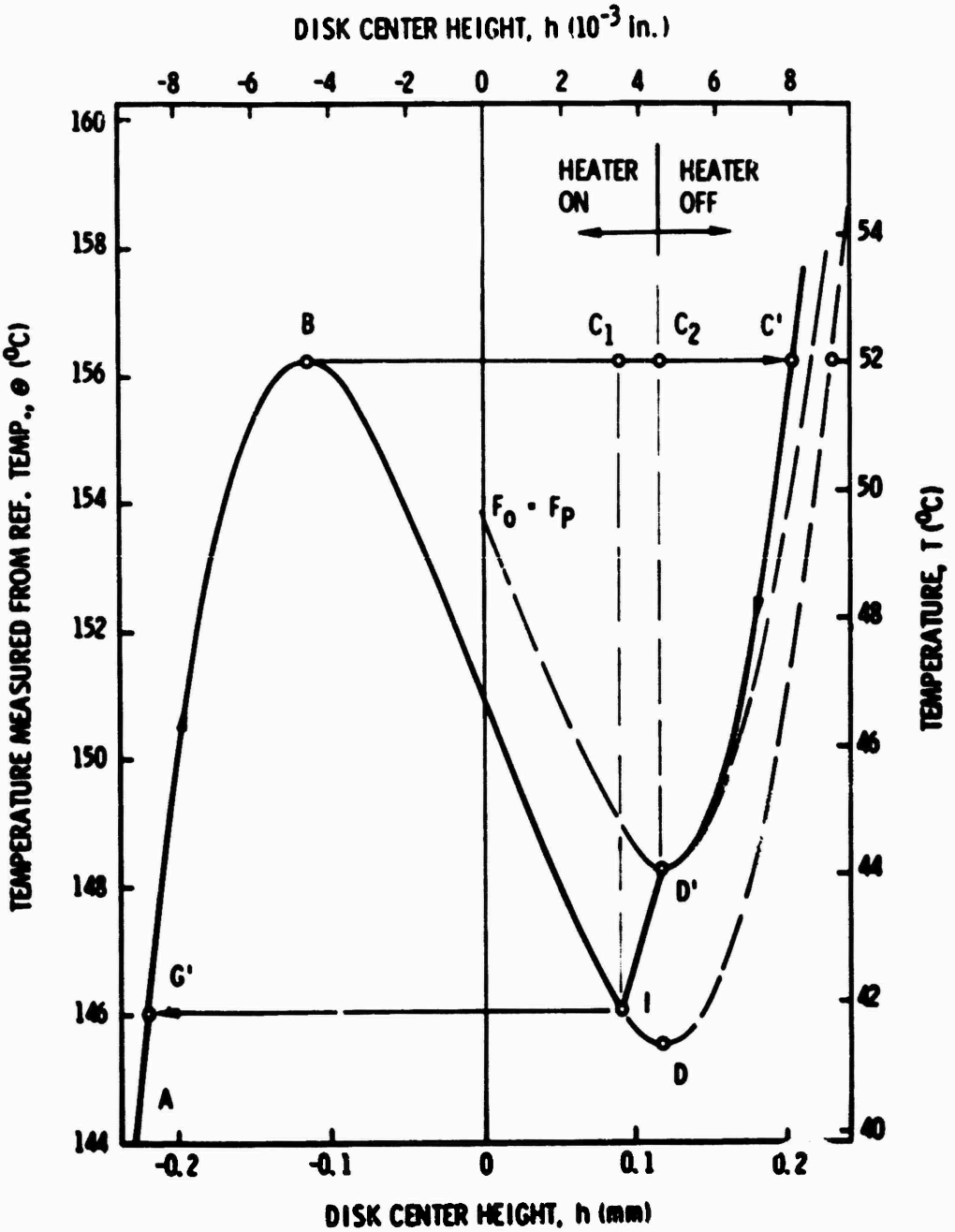

Fig. 6. Anomalous Switch—Creeping Type (temperature creepage near D')

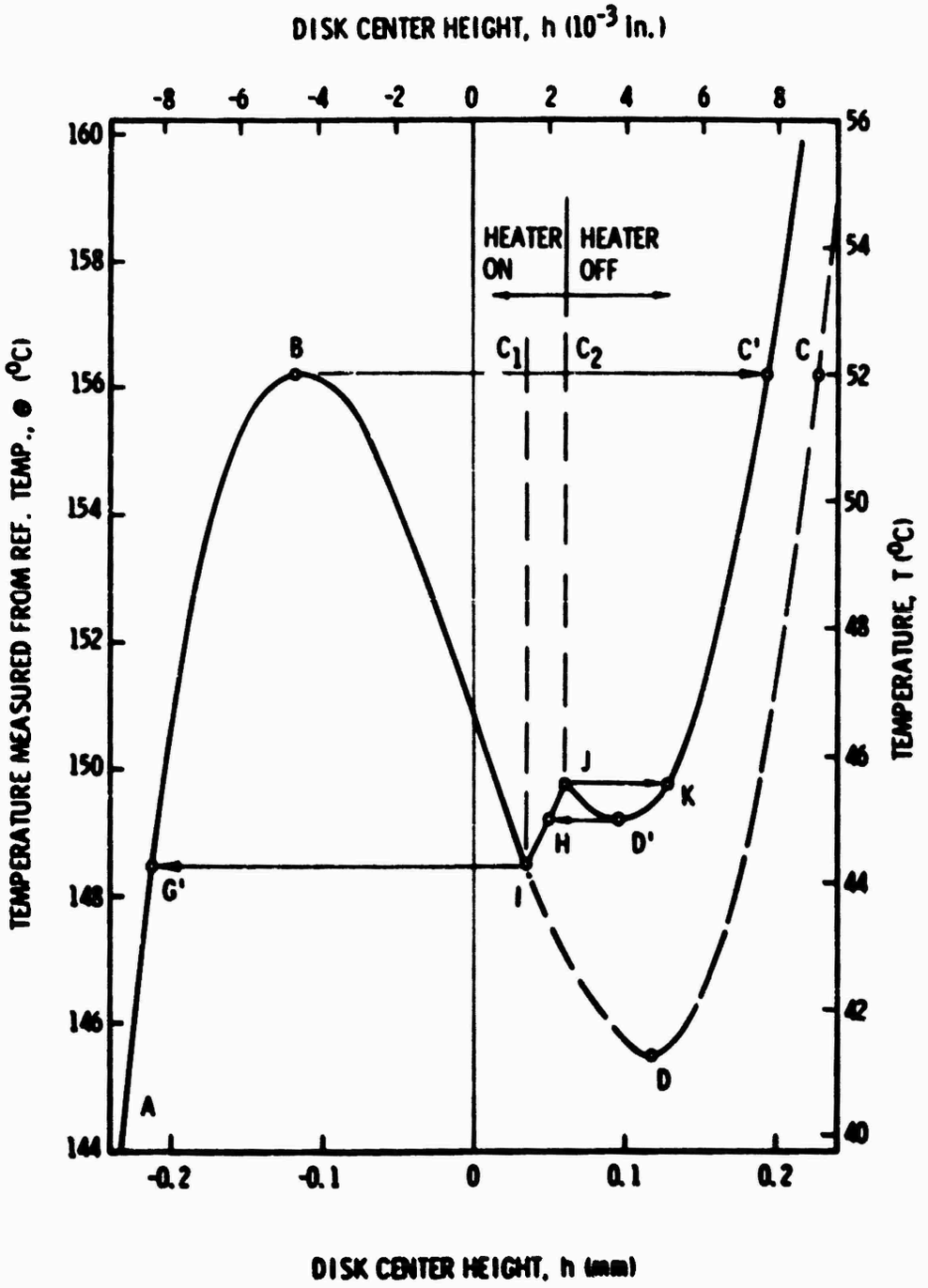

Fig. 7. Anomalous Switch—Dithering Type (note there exists a secondary switching loop KD'HJK)

The lower instability point D (see Fig. 7) is now within the temperature range of the transition segment IJ of the h-θ curve; therefore, when the disk is cooled from point C' to point D', it will move toward a stable "transition equilibrium state" H, at which the contacts are closed but the contact force is less than the set preload. If sufficient heat is transmitted from the heater to reverse the temperature decline before point I is reached, the disk temperature will rise toward point J along IHJ (see Fig. 7); at J the disk becomes unstable and moves to the stable equilibrium state K. This motion switches the heater off and causes the disk temperature to drop toward point D'. Thus, the thermostat may repeatedly perform the secondary switching cycle KD'HJK, which keeps the disk temperature "dithering" within a narrow range (about $0.6^{\circ}C$, as shown in Fig. 7) without letting the disk snap to a prebuckling configuration.

The above secondary switching loop cannot be completed if the disk temperature is controlled externally or if there is a sufficient time lag between contact closing and disk heating. In such cases, the disk temperature continues to drop along JHI until it reaches point I. At this point, the disk snaps to the prebuckling configuration G'and completes a primary (or designed) switching cycle G'BC'D'HIG'.

Figure 7 illustrates that, at a temperature within the dithering range (i.e., $149.14 < \theta < 149.73$), the disk-armature system has five equilibrium states. In order to investigate the stability of these equilibrium states, the values of the total strain energy at these states were calculated and are shown in Fig. 8. It was found that, during the secondary switching motions, the total strain energy varies by such a slight amount that an additional significant figure of accuracy was needed in the numerical calculations to obtain reasonable resolution. This indicates that during the secondary switching cycle, the disk-armature system is in a state of nearly neutral equilibrium if only the thermoelastic forces are present. Consequently, any effect that would be normally inconsequential in a stable-equilibrium region could assume an important role in the secondary switching cycle. Such factors as inertial forces due to shock or vibration, a slight asymmetry of the disk, material anisotropy, or electrostatic force due to voltage across the contacts could significantly alter the shape of the secondary switching cycle KD'HJK (see Fig. 7).

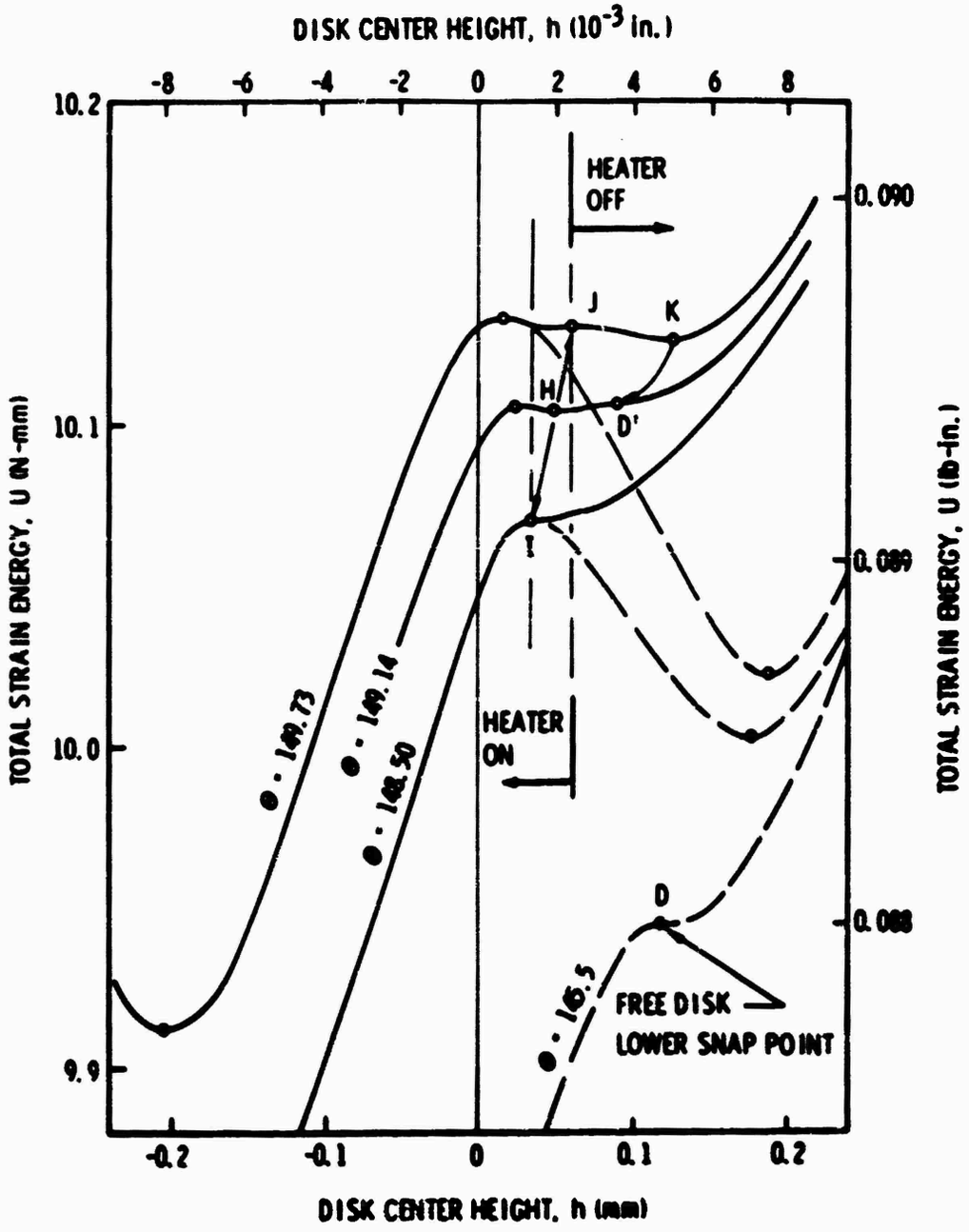

Fig. 8. Strain Energy in Free Disk (dashed lines) and in Disk-Armature System (solid lines)—Anomalous Switch (see Fig. 7)

VI. STRESSES IN BIMETALLIC DISK

It was shown in Ref. 3 that high mean and cyclic stresses may develop in a typical bimetallic disk during its thermal snap actions. Therefore, it is desirable to design a BMD thermostat with a view to limiting the maximum mean and cyclic stresses. Since Ref. 3 did not include the effects of the disk-pin interaction, a detailed investigation was performed in the present analysis to study whether this interaction force increases or decreases the severity of these stresses.

For normal thermostat behavior, illustrated in Figs. 4 and 5, the maximum cyclic stresses for both the free disk and the disk with pin-force are shown in Fig. 9 as functions of the disk temperature θ. These maximum cyclic stresses occur on the surfaces of the disk, at its center. It is significant to observe that the striker-pin force reduces the cyclic stress ranges of both material layers, evidently because it reduces the throw of the snap actions. Therefore, from the viewpoint of material fatigue damage, the presence of the disk-pin interaction force does not appear to increase the severity of the cyclic-stress problem from that of the baseline free disk.[3] It should be pointed out, however, that the above results are based on the assumption that the disk-pin interaction force is distributed over a finite area with a radius approximately equal to the disk thickness; in addition, the impact or dynamic effects of the snap action were neglected.

The maximum tensile stresses, which are usually the more critical factor in determining crack development in the material, are shown in Fig. 10 for the same disk, with and without the striker-pin force. These maximum tensile stresses occur at the edge of the disk as hoop stresses and always in material layer 2 (the low expansivity metal). Figure 10 indicates that the value of the maximum tensile stress is not affected by the presence of the disk-pin interaction, since it occurs just as the disk snaps past the flat position during both the upper and lower snap actions.

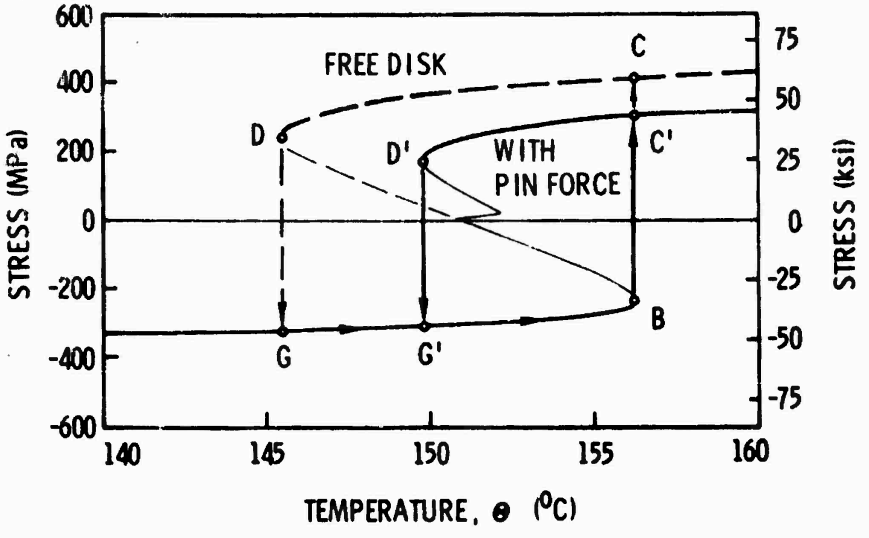

(a) Material 1 Surface Stress at Disk Center

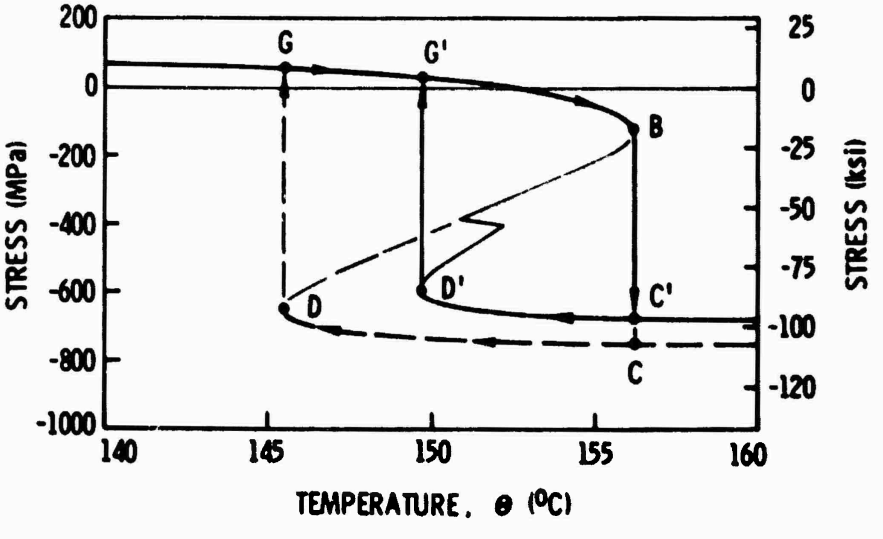

(b) Material 2 Surface Stress at Disk Center

Fig. 9. Comparison of Maximum Cyclic Stresses in Free Disk (dashed lines) and in Disk with Pin-Force (solid lines) --Normal Switch (see Fig. 4)

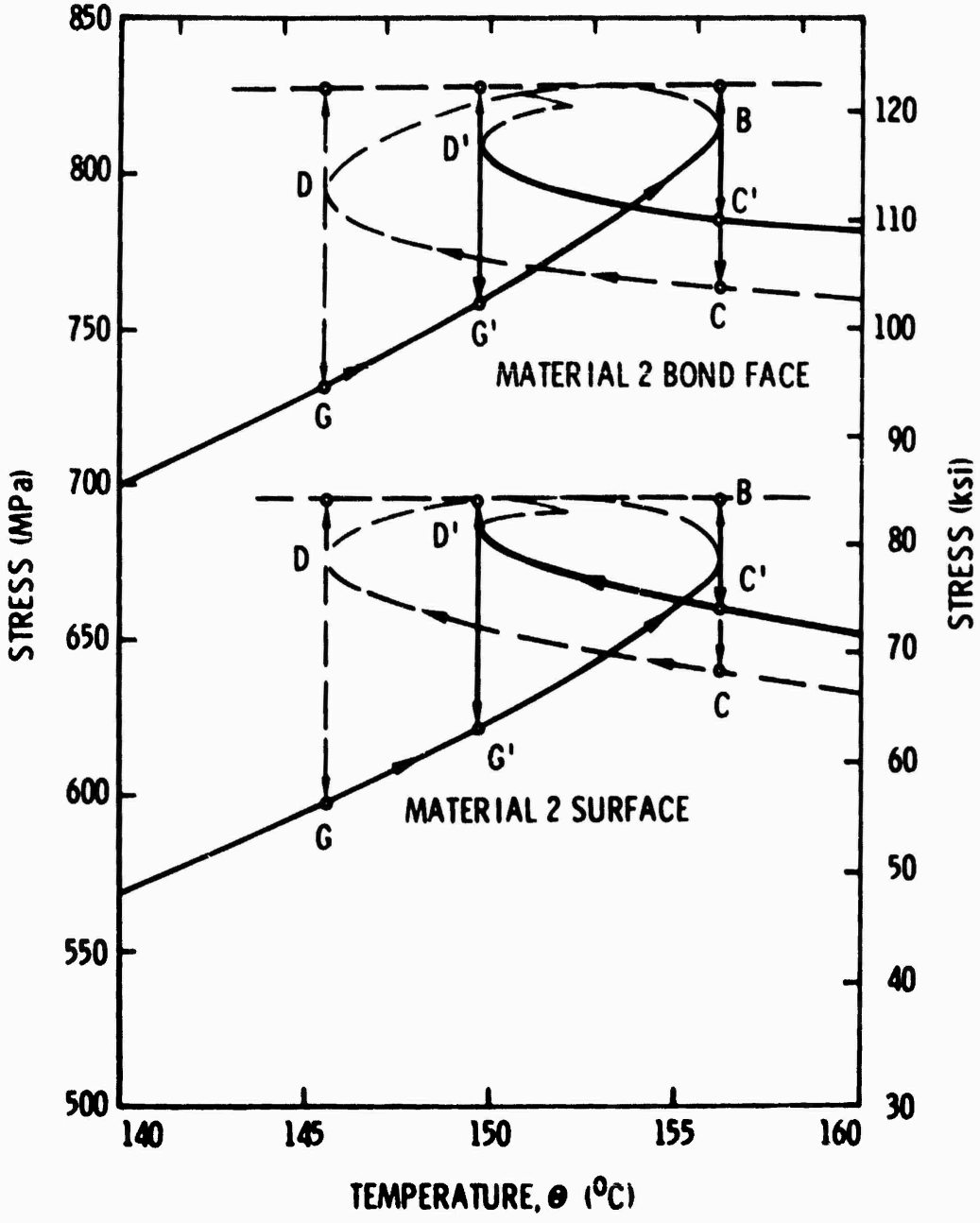

Fig. 10. Comparison of Maximum Tensile Stresses in Free Disk (dashed lines) and in Disk with Pin-Force (solid lines)--Normal Switch (see Fig. 4)

To summarize the effects of the striker-pin force on the disk stresses, it may be stated that, other than the possible transient effects due to disk-pin impact, the maximum tensile and cyclic stresses in the disk during the switching operation of a thermostat are bounded by those in the free disk during its snap cycle.

VII. CONSIDERATIONS FOR THERMOSTAT DESIGN IMPROVEMENT

From the above analysis, it may be seen that dithering or creepage of BMD thermostats results from a combination of the following three conditions:

1. A relatively high disk-pin interaction force F_p for the contact opening, creating a significant region of "transition" equilibrium (segment IJ of the curves shown in Figs. 4, 6 and 7)

2. A relatively short striker-pin, causing its disengagement from the disk at a position ($h = h_1$) that is close to the lower switching point

3. A slow rate of temperature change of the environment and a rapid thermal response of the switch-heater system, so the disk temperature does not experience appreciable overshoot from the switching temperatures

Among the above conditions, the last is partly imposed by the thermal environment and partly by a characteristic of the thermal system in which the thermostat is used; therefore, it cannot be eliminated by change of the thermostat design alone. Although it has recently been suggested that a delayed response, and thus an overshoot, of the thermostat temperature be purposely designed into the thermal system to eliminate temperature dithering, it is not a desirable solution for the following two reasons. First, for a given thermal capacitance between the heater and the thermostat, the temperature overshoot will be sufficient to prevent dithering only above a certain rate of temperature change; if the rate is slower, dithering will occur. Second, and more importantly, this technique only attempts to eliminate the "symptom" (the temperature dithering), but will not alleviate the underlying problem, i.e., the nearly neutral equilibrium and poor contact condition at the lower switching point. Therefore, improvement of the thermostat performance and reliability must be sought from design changes that eliminate the first two conditions above.

Condition 1 may be changed either by reducing the contact preload or by increasing the snap-temperature band $\Delta\Theta$ of the free disk (the latter does not necessarily imply an increased switching band of the thermostat). Since a sufficient contact preload is necessary to provide a good electrical contact and to prevent chattering, it does not appear promising that the contact preload in existing designs can be significantly reduced. Consequently, improvement can best be achieved by using bimetallic disks with wider snap-temperature band. From Fig. 4 and Eq. (35), it can be deduced that if $\Delta\Theta < 0.26\ (F_p/Q^*)$, the disk will always yield a bad switch. The following condition appears to provide a suitable criterion for the selection of bimetallic disks:

$$\Delta\Theta \geq 0.8\ (F_p/Q^*). \tag{36}$$

With the above selected values of $\Delta\Theta$, a normal switch should result if the disk-pin engagement point I shown in Fig. 4 is kept within the middle third of the temperature range $\Delta\Theta$.

Condition 2 above may be alleviated by maintaining a high dimensional precision for the parameter h_1 during the assembly of the thermostats or by selecting disks with increased throw of the snap actions so that the admissible range of h_1 is significantly increased. In order to ensure that the actual value of h_1 is well within the admissible range, detailed analysis should be performed for each thermostat design, and tolerance requirements for pertinent dimensions should be estimated and compared to practical limits. The following formulas, derived from a parametric study, enable one to calculate the initial disk center height h_o directly from the measured snap-temperature band $\Delta\Theta$ without going through the trial-and-error process mentioned above.

Let ξ denote a dimensionless parameter describing the initial disk center height, i.e.,

$$\xi = \frac{h_o}{h_{cr}} - 1 = \frac{\phi_o}{\phi_{cr}} - 1 \tag{37}$$

An extensive parametric study and curve fitting yield the following relation for the dimensionless quantity $(\tau_u - 1)$

$$(\tau_u - 1) = 1.07\xi^{3/2}(1 - 0.236\xi - 0.087\xi^2) \tag{38}$$

where $\tau_u = \theta_u/\theta_m$, as defined in Ref. 1. Equation (38) is valid for both a free disk and a disk with a small, constant central force, provided that h_o is within the scope of a shallow shell theory (say, $h_o < a/4$) and that the two Poisson's ratios ν_1 and ν_2 are not too widely different (say, $|\nu_1 - \nu_2| < 0.1$). In such cases, the two quantities $(1 - \tau_\ell)$ and $(\tau_u - 1)$ may be considered equal, and the snap-temperature band is given by the following relationship:

$$\Delta\theta = 2\theta_m(\tau_u - 1). \tag{39}$$

From Eq. (13), it may be readily shown that

$$\theta_m = \frac{(1+\nu_1)ED^3}{Q^3} \frac{2h_{cr}}{a^2}(1+\xi) \tag{40}$$

Substitution of Eqs. (38) and (40) into Eq. (39) yields

$$\Delta\theta = \frac{(1+\nu_1)ED^3h_{cr}}{Q^3a^2} 4.28\xi^{3/2}(1 + 0.764\xi - 0.323\xi^2 - 0.087\xi^3). \tag{41}$$

When the measured value of $\Delta\theta$ is known, Eq. (41) may be solved for the unknown parameter ξ, which may then be used in Eqs. (37) and (40) to calculate h_o and θ_m, respectively.

Finally, it is important to remark that a better understanding and control of the instability of the relevant material properties (e.g., those of INVAR are well known to be unstable) and alleviation of the residual stresses in the bimetallic disk must accompany any design-improvement effort; otherwise, any improvement in the switch performance and reliability achieved through design changes and dimensional precision can easily be negated by a drift in these material characteristics.

VIII. CONCLUSIONS

The analysis and numerical examples presented in this report provide a more detailed understanding of the operation of the BMD thermostat by including the effects of the disk-armature interaction force. It is shown that the temperature creepage or dithering caused by the anomalous switching actions of a miniaturized BMD thermostat may be attributed to the improper design of this interaction, and that these anomalies may escape detection in an acceptance test if the rate of change of the disk temperature is not sufficiently slow. A few theoretical guidelines have been suggested for design improvement.

SYMBOLS

a	radius of the edge of disk
B, C, D	disk constants defined in Ref. 1
D^*	$D - C^2/B$, equivalent bending rigidity of disk
E_1, E_2	Young's moduli of disk materials
e_r, e_θ	total strains in radial and circumferential directions
F, F_o	disk-striker-pin interaction force
F_p	the interaction force required to overcome contact preload
$h = \omega(o)$	disk center height measured from base-plane
$h_o = -\omega_o(o)$	initial disk center height (at stress-free state)
h_1	disk center height at striker-pin engagement position
M_r, M_θ	stress-couple resultants in disk
N_r, N_θ	stress resultants in disk
Q_r	transverse shear stress resultant in disk
r	radial distance from disk center
T	temperature
t	total thickness of disk
t_1, t_2	thickness of layers 1 and 2
U_d	strain energy in disk
U_{total}	total strain energy in disk-armature system
u	radial displacement of disk reference surface
w	axial distance from the reference surface of the disk to its base-plane

SYMBOLS (Continued)

w_e	axial displacement of disk reference surface
w_o	initial shape of the disk (at stress-free state)
α_1, α_2	coefficients of thermal expansion of disk materials
$\beta = dw_e/dr$	rotation of disk normal
$\epsilon_r, \epsilon_\theta$	elastic strains in radial and circumferential directions of disk reference surface
ζ	thickness coordinate, measured from reference (bond) surface of disk
λ	disk constant defined in Eq. (16)
ν_1, ν_2	Poisson's ratios of disk materials
ξ	$= (h_o/h_{cr}) - 1$, dimensionless parameter describing initial curvature
σ_r, σ_θ	stresses
$\tau = \theta/\theta_m$	dimensionless temperature parameter
ϕ, ϕ_o	variables describing the deformed and initial shapes of disk
θ	disk temperature measured from a reference temperature at its stress-free state
θ_u, θ_l	upper and lower snap temperatures of disk
θ_m	mean temperature of disk snap points
κ_r, κ_θ	changes of shell curvature

APPENDIX

SUMMARY OF WITTRICK'S DERIVATION

Consider a bimetallic disk of radius a and in the form of a shallow shell as shown in Fig. 3 (p. 14). The two layers, whose thicknesses are t_1 and t_2, whose Young's moduli are E_1 and E_2, and whose Poisson's ratios are ν_1 and ν_2, and having coefficients of linear thermal expansion α_1 and α_2, are assumed to be in perfect bond. Wittrick's basic assumption is that there exists a reference temperature, T_o, at which the disk is free from internal stresses and which has a slightly curved shape represented by the function $w_o(r)$. Other assumptions are that $t \ll a$ and that the magnitude of w_o is the same order as t, $(t = t_1 + t_2)$. Then, based on the large deflection theory of thin plates and shallow shells, the radial and circumferential strains may be expressed, respectively, as

$$\left.\begin{aligned} e_r &= \frac{d}{dr} + \frac{1}{2}\left(\frac{dw}{dr}\right)^2 - \frac{1}{2}\left(\frac{dw_o}{dr}\right)^2 - \zeta\left(\frac{d^2 w_e}{dr^2}\right) \\ e_\theta &= \frac{u}{r} - \frac{\zeta}{r}\frac{dw_e}{dr} \end{aligned}\right\} \qquad (A-1)$$

where u and w_e are the thermoelastic displacement components in r- and z-direction, respectively, of a point at a distance ζ from the reference (or bond) surface, and

$$w = w_o + w_e \qquad (A-2)$$

is the final (or deformed) shape of the disk.

Removal of the thermal strains due to a temperature change, $\theta = T - T_o$, gives the elastic strains due to stresses

$$e'_r = e_r - \alpha_i\theta, \qquad e'_\theta = e_\theta - \alpha_i\theta \qquad (A-3)$$

Note that α_i assumes the value α_1 for $\zeta > 0$, and α_2 for $\zeta < 0$. The radial and circumferential stresses are then given by

$$\sigma_r = \frac{E_i}{1 - \nu_i^2} (e'_r + \nu_i e') \tag{A-4}$$

$$\sigma_\theta = \frac{E_i}{1 - \nu_i^2} (e'_\theta + \nu_i e'_r) \tag{A-5}$$

Let N_r and N_θ be the radial and circumferential stress-resultants, respectively

$$N_r = \int_{-t_2}^{t_1} \sigma_r d\zeta, \qquad N_\theta = \int_{-t_2}^{t_1} \sigma_\theta \, d\zeta \tag{A-6}$$

and M_r and M_θ be the radial and circumferential stress-couple resultants, respectively

$$M_r = \int_{-t_2}^{t_1} \sigma_r \, d\zeta, \qquad M_\theta = \int_{-t_2}^{t_1} \sigma_\theta \, \zeta d\zeta \tag{A-7}$$

For a given disk, the following quantities were defined:

$$E'_1 = \frac{E_1}{1 - \nu_1^2}, \qquad E'_2 = \frac{E_2}{1 - \nu_2^2}.$$

$$B = E'_1 t_1 + E'_2 t_2, \qquad B' = \nu_1 E'_1 t_1 + \nu_2 E'_2 t_2.$$

$$C = \frac{1}{2}\left(E'_1 t_1^2 - E'_2 t_2^2\right), \qquad C' = \frac{1}{2}\left(\nu_1 E'_1 t_1^2 - \nu_2 E'_2 t_2^2\right).$$

$$D = \frac{1}{3}\left(E_1' t_1^3 + E_2' t_2^3\right), \qquad D' = \frac{1}{3}\left(\nu_1 E_1' t_1^3 + \nu_2 E_2' t_2^3\right),$$

$$P = \frac{\alpha_1 E_1 t_1}{1 - \nu_1} + \frac{\alpha_2 E_2 t_2}{1 - \nu_2}, \qquad Q = \frac{1}{2}\left(\frac{\alpha_1 E_1 t_1^2}{1 - \nu_1} - \frac{\alpha_2 E_2 t_2^2}{1 - \nu_2}\right). \tag{A-8}$$

Then, using Eqs. (A-1) through (A-5), Eq. (A-6) may be integrated to give

$$N_r = B\left[\frac{du}{dr} + \frac{1}{2}\left(\frac{dw}{dr}\right)^2 - \frac{1}{2}\left(\frac{dw_o}{dr}\right)^2\right] + B'\frac{u}{r} - P\theta - C\frac{d^2 w_e}{dr^2} - C'\frac{1}{r}\frac{dw_e}{dr} \tag{A-9}$$

$$N_\theta = B\frac{u}{r} + B'\left[\frac{du}{dr} + \frac{1}{2}\left(\frac{dw}{dr}\right)^2 - \frac{1}{2}\left(\frac{dw_o}{dr}\right)^2\right] - P\theta - C\frac{1}{r}\frac{dw_e}{dr} - C'\frac{d^2 w_e}{dr} \tag{A-10}$$

and Eq. (A-7) may be integrated to give

$$M_r = \frac{C}{B}N_r - \left(Q - \frac{PC}{B}\right)\theta - \left(D - \frac{C^2}{B}\right)\frac{d^2 w_e}{dr^2} - \left(D' - \frac{CC'}{B}\right)\frac{1}{r}\frac{dw_e}{dr} \tag{A-11}$$

$$M_\theta = \frac{C}{B}N_\theta - \left(Q - \frac{PC}{B}\right)\theta - \left(D - \frac{C^2}{B}\right)\frac{1}{r}\frac{dw_e}{dr} - \left(D' - \frac{CC'}{B}\right)\frac{d^2 w_e}{dr} \tag{A-12}$$

Equations (A-9) and (A-10) can be solved for u and (du/dr). Upon elimination of u, one obtains

$$B\left[N_r - \frac{d}{dr}(rN_\theta)\right] - B'\left[N_\theta - \frac{d}{dr}(rN_r)\right] = (BC' - B'C)\left[\frac{d}{dr}\left(r\frac{d^2 w_e}{dr^2}\right) - \frac{1}{r}\frac{dw_e}{dr}\right] + \frac{1}{2}(B^2 - B'^2)\left[\left(\frac{dw}{dr}\right)^2 - \left(\frac{dw_o}{dr}\right)^2\right] \tag{A-13}$$

In the absence of external forces, the equations of equilibrium are

$$\frac{d}{dr}(rN_r) - N_\theta = 0 \tag{A-14}$$

$$\frac{d}{dr}(rM_r) - M_\theta + rN_r\frac{dw}{dr} = 0 \tag{A-15}$$

Substitution of Eq. (A-14) into Eq. (A-13) gives

$$B\left[r^2\frac{d^2}{dr^2} + 3r\frac{d}{dr}\right]N_r + (BC'-B'C)\left[r\frac{d^2}{dr^2} + \frac{d}{dr} - \frac{1}{r}\right]\frac{dw_e}{dr}$$

$$= \frac{1}{2}(B^2-B'^2)\left[\left(\frac{dw_o}{dr}\right)^2 - \left(\frac{dw}{dr}\right)^2\right] \tag{A-16}$$

Also, substituting Eqs. (A-11) and (A-12) into Eq. (A-15) and using Eq. (A-14) gives

$$\left(D - \frac{C^2}{B}\right)\left[r\frac{d^2}{dr^2} + \frac{d}{dr} - \frac{1}{r}\right]\frac{dw_e}{dr} = rN_r\frac{dw}{dr} \tag{A-17}$$

Equations (A-16) and (A-17) are two coupled differential equations governing N_r and dw/dr.